

Range-Free Localization with the Radical Line

Hongyang Chen^{1,2}, Y. T. Chan³, H. Vincent Poor⁴, and Kaoru Sezaki^{1,2}

¹Institute of Industrial Science, The University of Tokyo, Tokyo, Japan

²CREST, JST, Japan

³Department of Electrical and Computer Engineering, Royal Military College of Canada, Kingston, Canada

⁴Department of Electrical Engineering, Princeton University, Princeton, NJ, USA

Email: hongyang@mcl.iis.u-tokyo.ac.jp, chan-yt@rmc.ca, poor@princeton.edu, sezaki@iis.u-tokyo.ac.jp

Abstract—Due to hardware and computational constraints, wireless sensor networks (WSNs) normally do not take measurements of time-of-arrival or time-difference-of-arrival for range-based localization. Instead, WSNs in some applications use range-free localization for simple but less accurate determination of sensor positions. A well-known algorithm for this purpose is the centroid algorithm. This paper presents a range-free localization technique based on the radical line of intersecting circles. This technique provides greater accuracy than the centroid algorithm, at the expense of a slight increase in computational load. Simulation results show that for the scenarios studied, the radical line method can give an approximately 2 to 30% increase in accuracy over the centroid algorithm, depending on whether or not the anchors have identical ranges, and on the value of DOI.

Index Terms—Wireless sensor networks, radical line, localization algorithm, centroid algorithm.

I. INTRODUCTION

A wireless sensor network (WSN) [1] typically consists of anchors and sensors communicating with each other. An anchor broadcasts its position coordinates, together with operating instructions, to the sensors. A sensor needs to determine its position to report to the anchors. Position determination can come from time-of-arrival, time-difference-of-arrival or angle-of-arrival measurements [2]. But when the sensors are low cost, low power and expandable units, with limited resources for computation, they often rely on range-free (RF) localization instead [3].

In RF localization, a sensor P determines its unknown position $P = [x, y]^T$ from N in-contact anchors a_i at known positions $a_i = [x_i, y_i]^T$ and having radio ranges $R_i, i = 1, \dots, N$. The sensor position must satisfy

$$\begin{aligned} \|P - a_i\|^{1/2} &= [(x - x_i)^2 + (y - y_i)^2]^{1/2} \\ &\leq R_i, \quad i = 1, 2, \dots, N. \end{aligned} \quad (1)$$

Solving (1) requires nonlinear programming, and there is not a unique answer. The Centroid Algorithm (CA) [3] gives a simple estimate $\hat{P} = [\hat{x}, \hat{y}]^T$, where

$$\hat{x} = \frac{\sum_{i=1}^N x_i}{N} \quad \text{and} \quad \hat{y} = \frac{\sum_{i=1}^N y_i}{N}. \quad (2)$$

But \hat{P} from (2) sometimes is outside the region of intersections (RI) of the circles centered at a_i with radii R , as defined by (1). For example, the \hat{P} in Fig. 1 is outside the RI (shaded area) of the three circles.

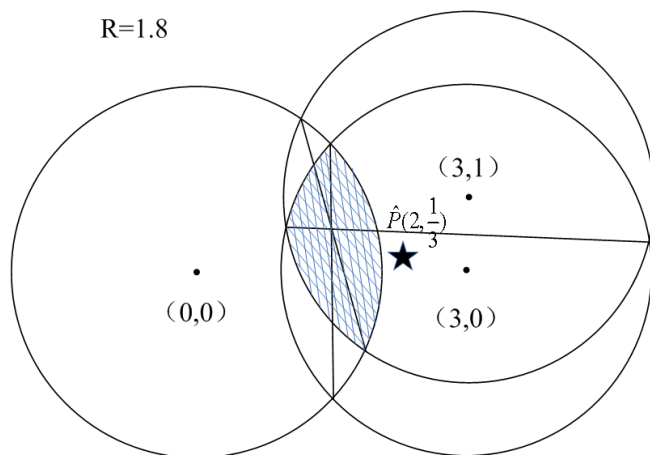


Fig. 1. The CA and radical line solutions

This paper proposes a new RF algorithm that has better accuracy than CA, but with a marginal increase in computations. However, the additional computations are well within the capability of present day sensors.

The line joining the intersection points of two circles is the radical line (RL) [4]. In Fig. 1, the RI contains a segment of the RL of any two circles, and the three RLs meet at a point inside the RI. Indeed, [4] proves that for three circles whose centers are not collinear, their three RLs always intersect at a point. Although sometimes this point can be outside the RI, it is inside in most cases.

In the following, Section II gives the development of the RL algorithm (RLA). Section III contains simulation results, which show that the RLA is more accurate than the CA, especially when the radii R_i are different. Conclusions are given in Section IV.

II. THE RADICAL LINE ALGORITHM

In WSNs, a sensor can determine whether it is in the transmission range of an anchor node according to the beacon signal received from the anchor. Most literature on range-free localization assume a nominal range (or detection range) R , i.e., an anchor can communicate with a sensor within R meters from it. However, the actual range in practice is dependent on the propagation conditions. A measure of the variation in range

coverage is the degree of irregularity (DOI). Its value denotes the maximum range variation per unit degree change in the direction of radio propagation. Recently, [5] gives a condition required for a successful anchor-to-sensor contact. Let $W(a_i)$ be the power received by a sensor from a_i , Q be the ambient noise power, and S the interference power in the WSNs. Then there is a contact only if

$$\frac{W(a_i)}{Q + S} \geq TH, \quad (3)$$

where TH is a hardware dependent threshold.

Let a sensor P be at an unknown position $P = [x, y]^T$, in contact with N anchors a_i at known positions $a_i = [x_i, y_i]^T$ and having radio ranges R_i . Hence P must lie in the RI of the N circles, centered at a_i with radii R_i . Depending on N , there are three cases to consider.

A. $N > 3$

For N circles, there are $\frac{N!}{2^{!(N-2)!}}$ RLS. To reduce computations, RLA selects only the RLS of the two circles whose centers are separated by the largest distance among the N circles. The idea behind this choice is that the RL of these two circles will be the shortest, and hence their RL has the highest probability of appearing inside the RI of all the N circles.

Let

$$d_{ij} = \|a_i - a_j\|^{1/2} = d_{ji}, \quad i, j = 1, \dots, N \quad (4)$$

be the distance between the centers of a_i and a_j and let d_{qk} be the maximum of the values in (4). For illustration simplicity, let $q = 1$, and $k = 2$. Referring to Fig. 2, the end points of the RL are $I_a = [x_a, y_a]^T$ and $I_b = [x_b, y_b]^T$, and $O = [x_o, y_o]^T$ is the intersection between the RL and the line joining a_1 and a_2 .

Let

$$d_{o1} = \|O - a_1\|^{1/2} \quad (5)$$

and

$$d_{o2} = \|O - a_2\|^{1/2}. \quad (6)$$

It follows that

$$d_{o1}^2 + m^2 = R_1^2 \quad (7)$$

and

$$d_{o2}^2 + m^2 = R_2^2. \quad (8)$$

Subtracting (8) from (7) gives

$$2(x_2 - x_1)x_o + 2(y_2 - y_1)y_o = R_1^2 - R_2^2 + k_2 - k_1, \quad (9)$$

where

$$k_i = x_i^2 + y_i^2. \quad (10)$$

Further, equating the slopes of the a_1 to O and a_2 to a_1 lines in Fig. 2 yields

$$\frac{y_2 - y_o}{x_2 - x_o} = \frac{y_2 - y_1}{x_2 - x_1}, \quad (11)$$

giving

$$(y_2 - y_1)x_o - (x_2 - x_1)y_o = x_2(y_2 - y_1) - y_2(x_2 - x_1). \quad (12)$$

Solving (9) and (12) then gives $O(x_o, y_o)$.

Let $d_{12} = D$. Then

$$R_1^2 - d_{o1}^2 = m^2 = R_2^2 - (D - d_{o1})^2, \quad (13)$$

so that

$$d_{o1} = \frac{R_1^2 - R_2^2 + D^2}{2D} \quad (14)$$

and

$$m = (R_1^2 - d_{o1}^2)^{1/2}. \quad (15)$$

Now in Fig. 2, the following trigonometric relations hold:

$$\frac{x_o - x_a}{m} = \frac{y_o - y_1}{d_{o1}} \quad (16)$$

and

$$\frac{y_o - y_a}{m} = \frac{x_o - x_1}{d_{o1}}. \quad (17)$$

From (16) and (17), the coordinates for I_a are

$$x_a = x_o - \frac{m}{d_{o1}}(y_o - y_1) \quad (18)$$

and

$$y_a = y_o + \frac{m}{d_{o1}}(x_o - x_1). \quad (19)$$

Following the same procedure gives

$$x_b = x_o + \frac{m}{d_{o1}}(y_o - y_1) \quad (20)$$

and

$$y_b = y_o - \frac{m}{d_{o1}}(x_o - x_1). \quad (21)$$

Next, RLA selects L test points $t_l = [x_l, y_l]^T$, $l = 1, \dots, L$, on RL, by taking equal increments between I_a and I_b to give

$$x_l = x_a + \frac{l(x_b - x_a)}{L + 1} \quad (22)$$

and

$$y_l = y_a + \frac{l(y_b - y_a)}{L + 1}. \quad (23)$$

L is a user parameter, depending on the resolution required. In the simulation experiment in Section III, $L = 4$. At each t_l , RLA checks whether t_l is inside the RI, and if not, how far away from the RI it is, by computing the error

$$\varepsilon_{li} = \|t_l - a_i\|^{1/2} - R_i = \begin{cases} \varepsilon_{li} & \text{if } \varepsilon_{li} > 0 \\ 0 & \text{if } \varepsilon_{li} \leq 0 \end{cases} \quad (24)$$

and then summing the errors over all a_i to give

$$S_l = \sum_{i=1}^N \varepsilon_{li}. \quad (25)$$

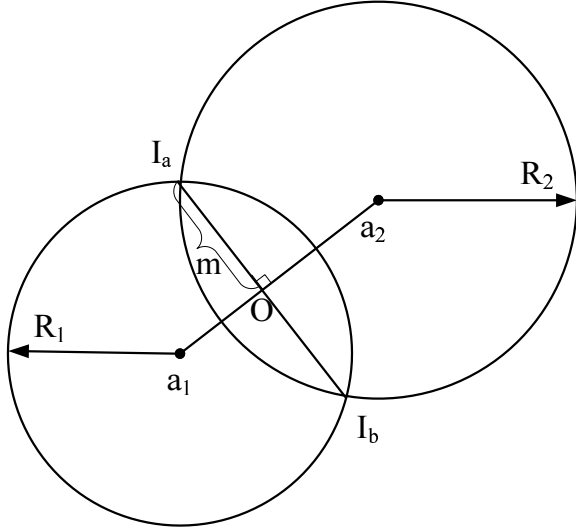


Fig. 2. The end points of an RL

If an $S_l = 0$, the corresponding t_l is inside the RI and is the estimate for P . If all $S_l > 0$, the RL is not inside the RI of the N circles. It is then necessary to compute the CA errors

$$S_c = \sum_{i=1}^N \varepsilon_{ci} \quad (26)$$

where ε_{ci} comes from (24), with $c = [\hat{x}, \hat{y}]^T$ from (2) replacing t_l . The final estimate for P , \hat{P} , comes from choosing the t_l or c , whose corresponding S_l or S_c is the minimum.

B. $N = 2$ and $N = 3$

When $N = 2$, \hat{P} is the same as $O(x_o, y_o)$. When $N = 3$, RLA computes the intersection of the three RIs. Let that intersection point be $I = [x_I, y_I]^T$. Extending Fig. 2 to three circles yields

$$(x_I - x_i)^2 + (y_I - y_i)^2 + h^2 = R_i^2, \quad i = 1, 2, 3 \quad (27)$$

where $h^2 \leq m^2$. Subtracting this expression for $i = 2, 3$ from that for $i = 1$ results in

$$AI = b \quad (28)$$

where

$$A = \begin{bmatrix} x_2 - x_1 & y_2 - y_1 \\ x_3 - x_1 & y_3 - y_1 \end{bmatrix}, \quad (29)$$

$$\text{and } b = \frac{1}{2} \begin{bmatrix} k_2 - k_1 + R_1^2 - R_2^2 \\ k_3 - k_1 + R_1^2 - R_3^2 \end{bmatrix}. \quad (30)$$

Solving (28) gives

$$I = A^{-1}b. \quad (31)$$

If the determinant of A equals 0, then the three circles are collinear. Or if $\|I - a_i\|^{1/2} > R_i$ for any i , then I is outside the RI. For these two cases, RLA takes the centroid of the two circles with the largest separation as \hat{P} .

III. SIMULATION RESULTS

In the simulation experiments, the WSN has an area of 100 m x 100 m, and contains 100 randomly placed (different for each trial) sensors. For a given number of anchors (NA), occupying random (different for each trial) but known positions, the number of anchors N in contact with an arbitrary sensor can vary from 2 to NA. Some anchors have $R = R_{max} = 45m$, and some have $R = 0.5R_{max}$. The localization errors decrease with increasing NA. For 100 independent trials, the error as a fraction of R_{max} is

$$e(NA) = \frac{1}{100} \sum_{j=1}^{100} \left\{ \frac{\sum_{i=1}^{100} \|p_j(i) - \hat{p}_j(i)\|^{1/2}}{100R_{max}} \right\}. \quad (32)$$

In (32), $p_j(i)$ is the true i th sensor position at trial j , and $\hat{p}_j(i)$ is its estimate.

In an experiment where $DOI = 0$, a sensor that lies within the nominal R_i of an anchor is in contact with that anchor. When $DOI \neq 0$, the actual R_i is smaller, given by $R_i(DOI) = R_i(1 - DOI)$.

Fig. 3 plots $e(NA)$ for both CA and RLA with all anchors' $R = R_{max}$ and as NA varies from 24 to 36, at a $DOI = 0$. The results show that RLA has lower $e(NA)$ than CA.

Fig. 4 plots $e(NA)$ for both CA and RLA and all $R = R_{max}$ as NA varies from 24 to 36, at a $DOI = 0.1$. The results show that RLA has lower $e(NA)$ than CA.

Fig. 5 plots $e(NA)$ for both CA and RLA with different transmission ranges, i.e., some a_i have $R = R_{max} = 45m$ and some have $R = 0.5R_{max}$ as NA varies from 24 to 36, at a $DOI = 0$. The improvement of RLA over CA is more significant than when all anchors have $R = R_{max}$.

Fig. 6 plots $e(NA)$ for both CA and RLA with different transmission ranges as NA varies from 24 to 36, at a $DOI = 0.2$. A comparison of the errors in Figs. 4-6 reveals that RLA has increasing accuracy over CA, when DOI increases. The improvement is more significant when the anchors have different ranges.

Fig. 7 is a snapshot of one trial in the anchor-sensor geometry with $NA = 30$ and different transmission ranges, together with the placement of \hat{P} . A dotted line joins P to \hat{P} . Comparing Fig. 7(a) to Fig. 7(b), the dotted lines for RLA are generally shorter than those for CA.

Fig. 8 plots $e(NA)$ for both CA and RLA as the number of sensors varies from 50 to 80 with the same transmission range, at $DOI = 0.1$. The number of anchors $NA = 30$.

Fig. 9 plots $e(NA)$ for both CA and RLA as the number of sensors varies from 50 to 80 with different transmission ranges, at $DOI = 0.1$. The number of anchors $NA = 30$. Comparing Fig. 8 with Fig. 9 shows that the accuracy gain of RLA over CA is higher when the anchors have different ranges, than when they have the same range.

IV. CONCLUSIONS

Range-free localization, while not as accurate as range-based, has the principal advantage of simplicity, i.e., there is

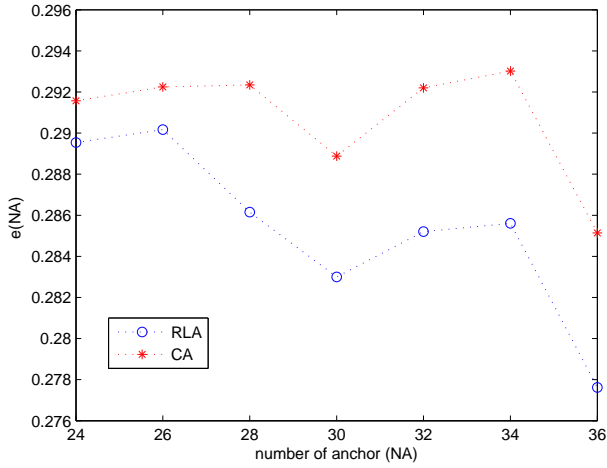


Fig. 3. The average localization error vs. the number of anchors (DOI=0 and the same transmission range)

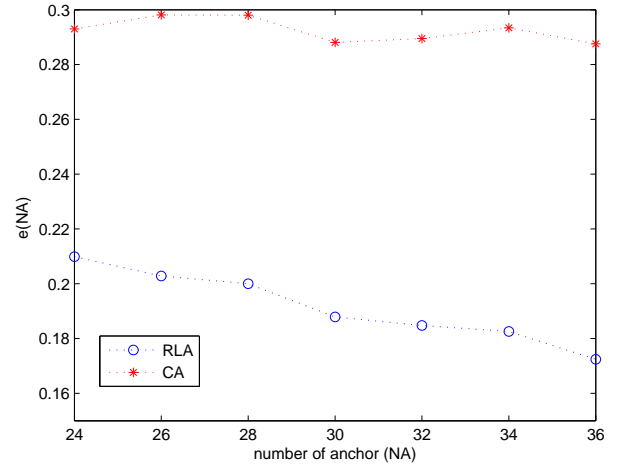


Fig. 5. The average localization error vs. the number of anchors (DOI=0 and different transmission ranges)

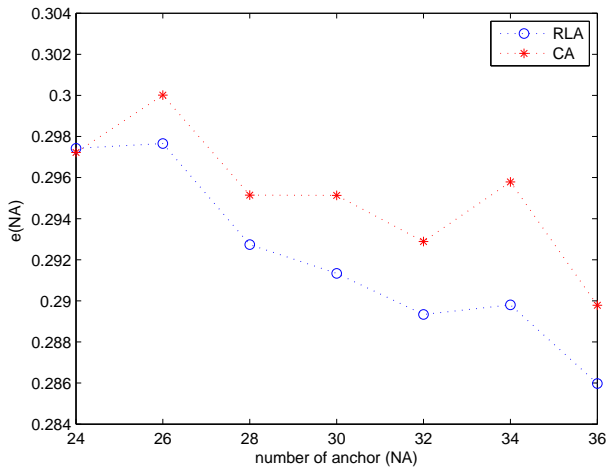


Fig. 4. The average localization error vs. the number of anchors (DOI=0.1 and the same transmission range)

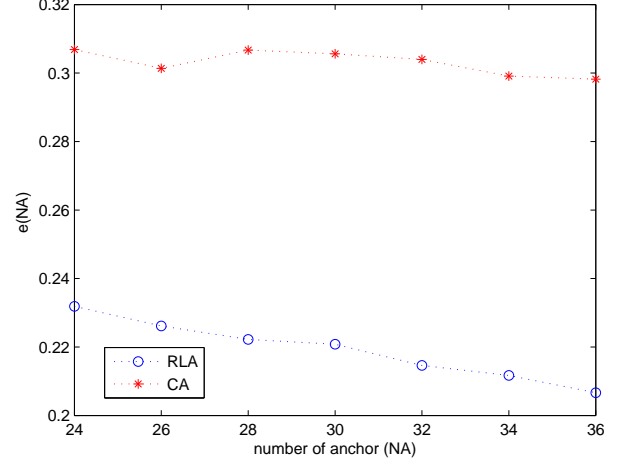


Fig. 6. The average localization error vs. the number of anchors (DOI=0.2 and different transmission ranges)

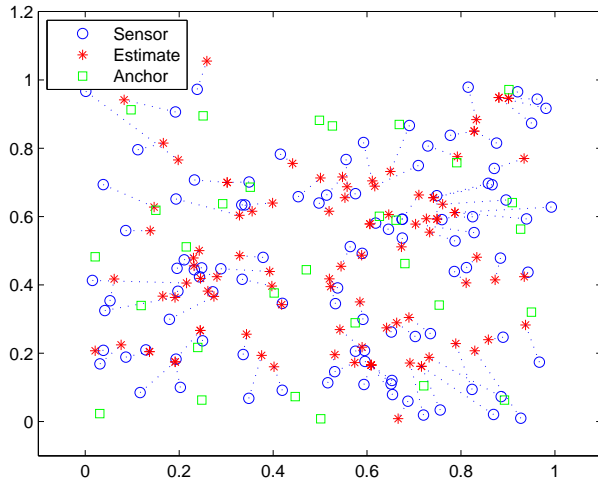
no requirement for special hardware to measure time-of-arrival or time-difference-of-arrival. This is important for WSN in which sensors are low cost units, and in some applications where knowing accurate sensor positions is not critical. While determining \hat{P} from CA is simple, it is possible to improve on its accuracy with some additional computations. The RLA provides such an option and the simulation results in Section III show that there is approximately a 2 to 30% gain in accuracy, depending on whether or not the anchors have identical ranges, and on the value of DOI.

ACKNOWLEDGEMENT

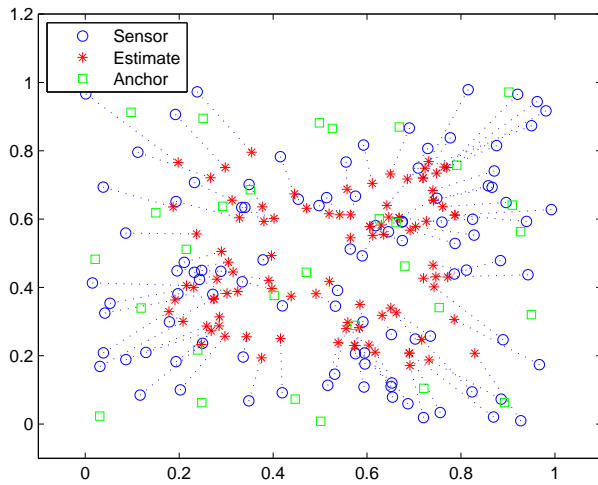
This work was supported by the CREST Advanced Integrated Sensing Technology project of the Japan Science and Technology Agency.

REFERENCES

- [1] T. He, C. Huang, B. M. Blum, J. A. Stankovic, and T. Abdelzaher, "Range-free localization schemes for large scale sensor networks," in *Proc. ACM MobiCom*, San Diego, CA, Sept. 2003, pp. 81-95.
- [2] J. Luo, H. V. Shukla, and J.-P. Hubaux, "Non-interactive location surveying for sensor networks with mobility-differentiated ToA," in *Proc. IEEE INFOCOM*, Barcelona, Spain, Apr. 2006, pp. 1-12.
- [3] N. Bulusu, J. Heidemann, and D. Estrin, "GPS-less low-cost outdoor localization for very small devices," *IEEE Personal Comm. Magazine*, vol. 7, no. 5, pp. 28-34, Oct. 2000.
- [4] H. S. M. Coxeter, *Introduction to Geometry*. New York: Wiley, 1969.
- [5] T. Moscibroda, R. Wattenhofer, and A. Zollinger, "Topology control meets SINR: The scheduling complexity of arbitrary topologies," in *Proc. MobiHoc'06*, Florence, Italy, May 2006, pp. 310-321.



(a) Localization error of RLA (DOI=0.1, error = 0.1929)



(b) Localization error of CA (DOI=0.1, error = 0.2872)

Fig. 7. Location error with different transmission ranges

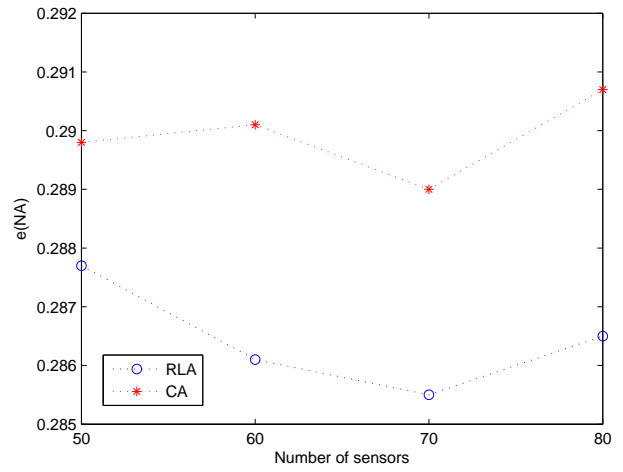


Fig. 8. The average localization error vs. the number of sensors (DOI=0.1 and the same transmission range)

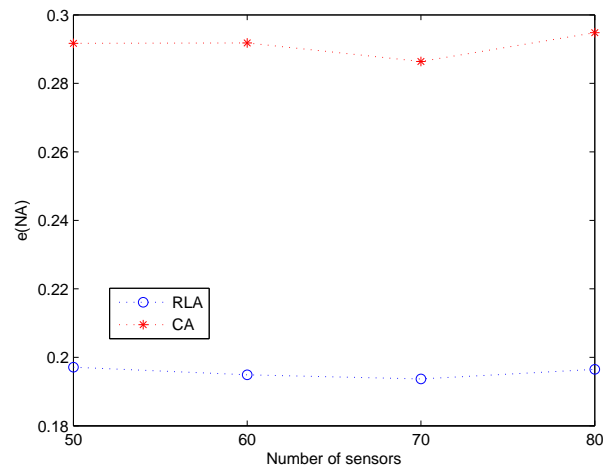


Fig. 9. The average localization error vs. the number of sensors (DOI=0.1 and different transmission ranges)